# Angular dependence of the ion-induced secondary-electron yield from solids

B. Svensson, G. Holmén, and A. Burén
*Department of Physics, Chalmers University of Technology, S-412 96 Göteborg, Sweden*
(Received 17 February 1981)

The secondary-electron yield from polycrystalline copper induced by protons, noble-gas ions, and copper ions has been studied as a function of angle of ion incidence in the range 0° to 85°. The experimental results are explained in terms of a recently developed theory for secondary-electron emission. The kinetic emission of electrons is regarded as consisting of two parts which exhibit different dependences on the angle of ion incidence. Good agreement is found between theory and experiment.

## I. INTRODUCTION

When particles penetrate solid matter, they lose energy and slow down. A vast number of secondary processes may take place, such as emission of photons and electrons, sputtering of target atoms and displacement of target atoms, nuclear reactions, and chemical reactions.

In the present work the emission of electrons has been studied. Usually a distinction is made between potential and kinetic emission. The former is due to neutralization of the impinging ion before it reaches the surface. The latter is caused by ionizing collisions in the target material. In the following, only cases where potential emission plays a minor role are considered.[1] The present paper gives further proof of the fact that the number of emitted electrons is proportional to the amount of energy deposited in electronic excitation near the target surface, as was suggested in earlier papers.[1-3]

## II. EXPERIMENTAL

The angular dependence of the secondary-electron yield has been measured using polycrystalline copper bombarded by protons, noble gas ions, and copper ions in the angular range 0° to 70° at ion energies between 30 and 400 keV. At energies below 50 keV the measurements have been extended to 85°.

The 50-kV isotope separator and the 400-kV ion accelerator at our laboratory have been used to bombard the copper target placed in an ultrahigh-vacuum system connected to the accelerators. The experimental system is described in detail elsewhere.[1,4,5] Target dimensions were $10 \times 10$ mm$^2$ with a thickness of 1 mm, except for the measurements in the angular range 0° to 85° where a $10 \times 45$ mm$^2$ target was used. Measurements were performed with two different qualities of polycrystalline copper: (1) FIN copper (with a grain size of 20–100 $\mu$m), used at ion energies below 80 keV, and (2) GB copper (70–300 $\mu$m), used at energies over 80 keV. A detailed discussion about the target materials is given in Ref. 1.

The same target treatment, the same experimental procedure, and similar experimental conditions as reported in Ref. 1 were maintained throughout all the present series of measurements.

## III. RESULTS

### A. Variation with ion mass and energy

In order to compare the angular dependence of the electron yield for different kinds of bombarding ions and at different ion energies, the experimental curves are fitted by a relation of the form

$$\gamma_{\text{expt}}(\phi) = \gamma_{\text{expt}}(0)(\cos\phi)^{-z} , \quad (1)$$

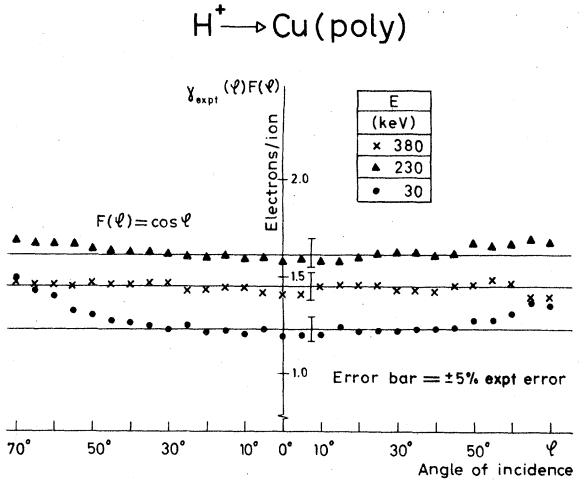


FIG. 1. Reduced secondary-electron yield as a function of the angle of incidence for protons on copper.

 

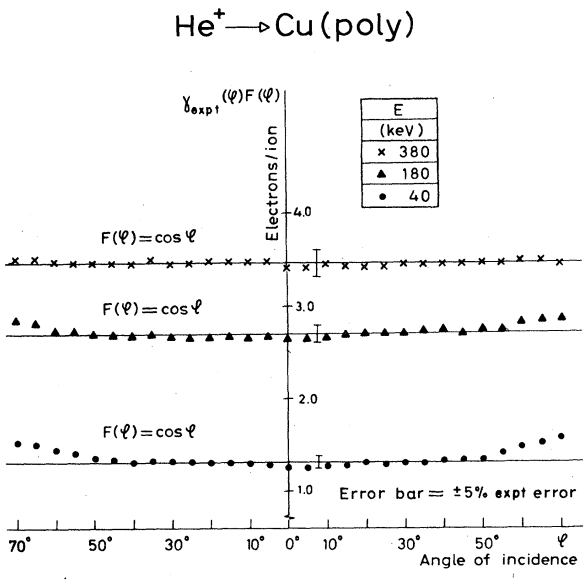


FIG. 2. Reduced secondary-electron yield as a function of the angle of incidence for helium ions on copper.

where $\phi$ is the angle of ion incidence and $z$ is a fitting parameter. For the different kinds of ions used $\gamma_{expt}(\phi)(\cos\phi)^z$, written $\gamma_{expt}(\phi)F(\phi)$, is plotted versus $\phi$ with ion energy as a parameter (Figs. 1–6). For protons and helium ions (Figs. 1 and 2, respectively), $z=1.0$ is a good approximation. For neon

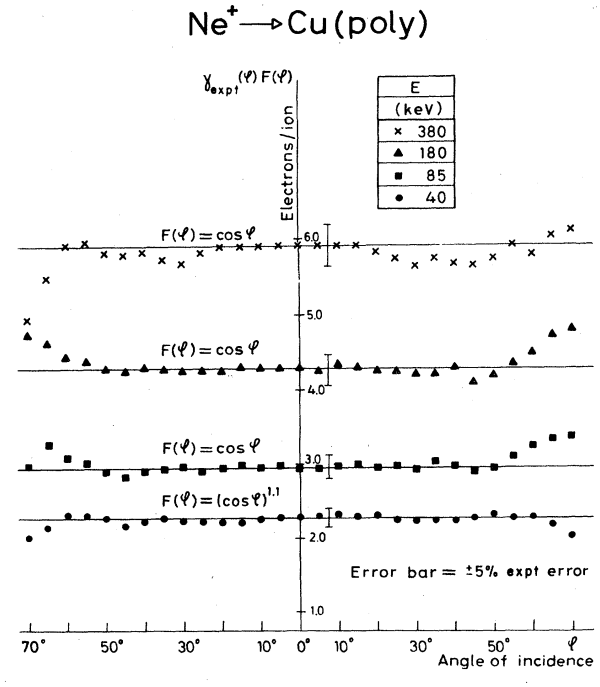


FIG. 3. Reduced secondary-electron yield as a function of the angle of incidence for neon ions on copper.

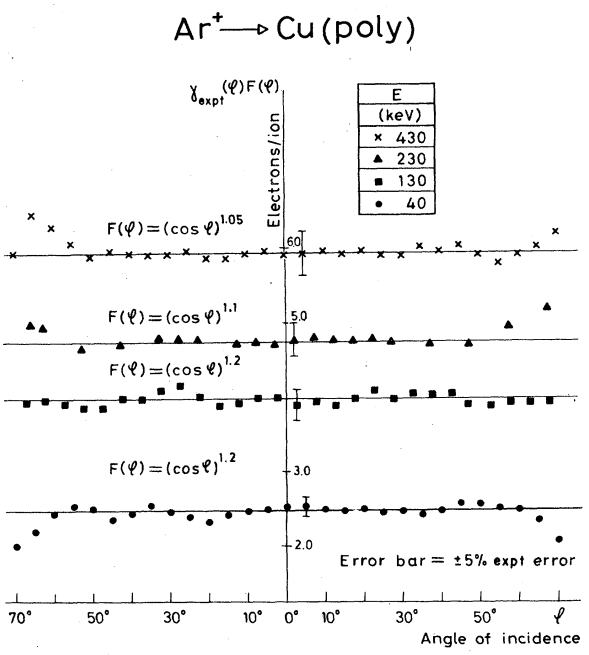


FIG. 4. Reduced secondary-electron yield as a function of the angle of incidence for argon ions on copper.

ions (Fig. 3) $z=1.0$ is an acceptable approximation at energies $\gtrsim 85$ keV, while at 40 keV $z=1.1$ gives the best fit. For argon and krypton ions $z$ increases from $\sim 1.05$ to 1.20 as the ion energy decreases (Figs. 4 and 5). If xenon ions are used, $z$ goes from 1.5 at 40 keV to 1.2 at 400 keV (Fig. 6). Deviations from Eq.

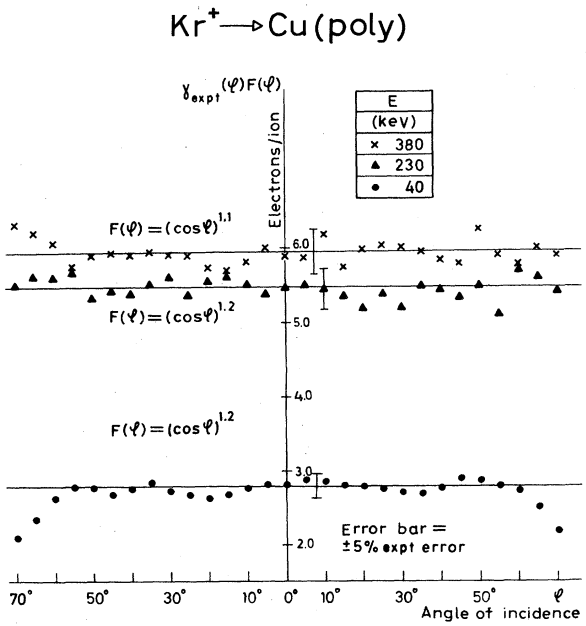


FIG. 5. Reduced secondary-electron yield as a function of the angle of incidence for krypton ions on copper.

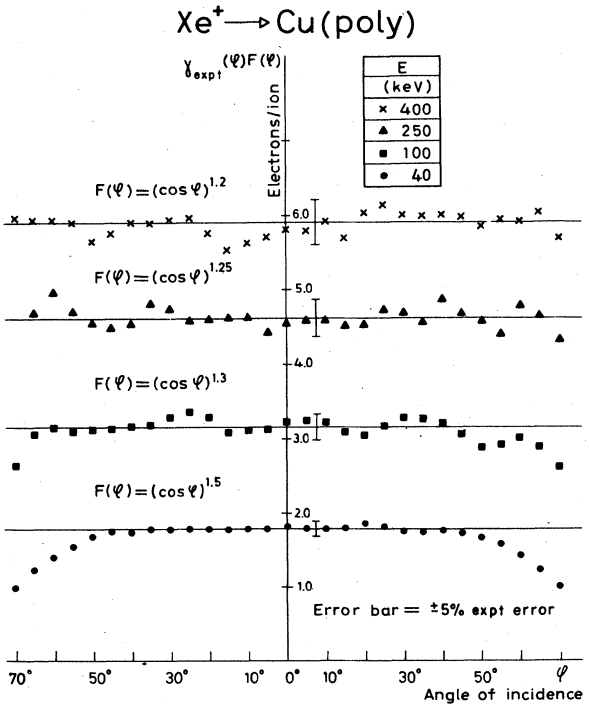


FIG. 6. Reduced secondary-electron yield as a function of the angle of incidence for xenon ions on copper.

(1) larger than may be explained by the experimental error are found in the range $50° \lesssim \phi \lesssim 70°$ at low ion energies, 30–40 keV. For protons and helium ions the $z$ value increases with angle, while for the heavier ions it decreases.

### B. Secondary-electron yield maxima

Figure 7 shows the measured yield versus the angle of ion incidence for 40-keV ions of neon, argon, copper, krypton, and xenon. The angle has here been extended to 85°. Maxima were obtained around 80° for xenon ions, 82° for krypton and copper ions, and 83° for argon ions. The neon curve indicates a maximum at about 85°. When 40-keV helium ions and protons were used, no such maxima could be reached even at 85°.

## IV. SUMMARY

The results of the measurements can be summarized as follows.

### A. Light-ion bombardment

(1) No variation of the fitting exponent $z$ with ion energy has been found. (2) An inverse cosine is a

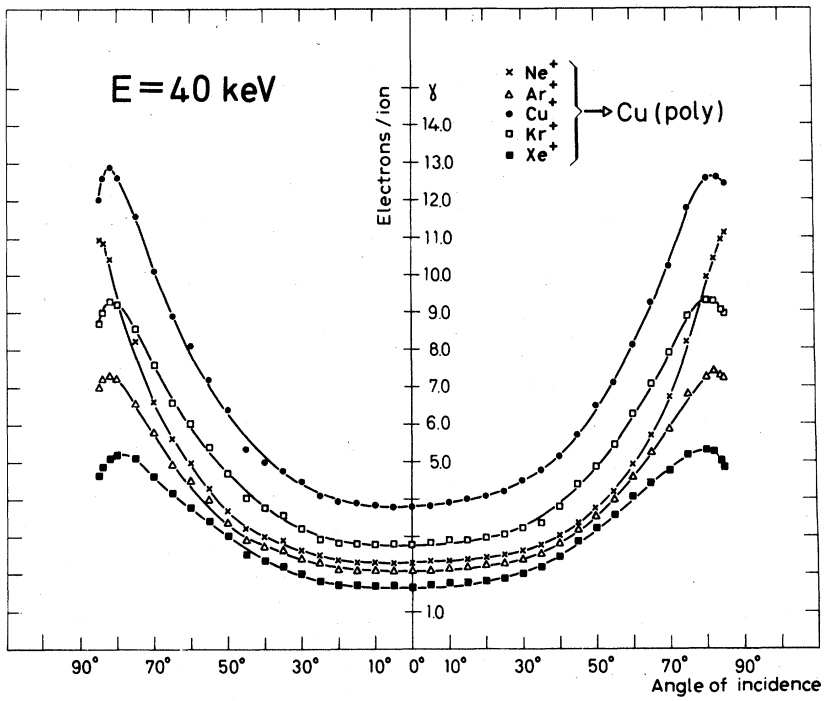


FIG. 7. Secondary-electron yield as a function of angle of ion incidence for 40-keV ions of neon, argon, copper, krypton, and xenon.

good approximation. (3) No maximum has been observed below 85°.

### B. Medium- and heavy-ion bombardment

(1) A variation of the angular dependence with ion mass and ion energy has been found. (2) An inverse cosine dependence underestimates the electron yield. (3) A maximum has been observed, within the angular range $80° \lesssim \phi \lesssim 85°$, slightly dependent on the kind of incident ion.

## V. THEORY

Most of the available theories for ion-induced electron emission from solids deal with how the electron yield depends on ion energy, and only small efforts have been made to deduce the variation with angle of ion incidence.

A theoretical treatment is made here of the angular dependence in terms of a recently developed theory for electron emission.[2,3] The following relation for the secondary electron yield, $\gamma$, is used as a starting point,

$$\gamma = \Lambda D(x=0,E,\cos\phi) \ , \tag{2}$$

where $\Lambda$ is a constant determined by properties of the target material, $D(x=0,E,\cos\phi)$ the mean energy per unit depth deposited in electronic excitation at the surface by a bombarding ion, $x$ the depth inside the target, $E$ the initial ion energy, and $\phi$ the angle of ion incidence.

As $\Lambda$ is assumed to be independent of $\phi$, the angular dependence, normalized to the yield at perpendicular incidence, can be expressed in the form

$$\frac{\gamma(\phi)}{\gamma(0)} = \frac{D(0,E,\cos\phi)}{D(0,E,1)} \ . \tag{3}$$

In order to determine $D$ the contributions due to electronic and nuclear stopping of the incoming ion are separated,[2,6] according to

$$D(x,E,\cos\phi) = D_{(p)}(x,E,\cos\phi) + D_{(r)}(x,E,\cos\phi) \ , \tag{4}$$

where $D_{(p)}$ is the mean energy per unit depth deposited primarily in electronic excitation by the bombarding ion, and $D_{(r)}$ is the mean energy per unit depth deposited in electronic excitation by recoiling target atoms.

In the evaluation of $D_{(p)}$ and $D_{(r)}$ the following approximations are made: (1) Energy transport by excited electrons is ignored. (2) The target is considered to be imbedded in an inifinite medium with a reference plane at $x=0$, i.e., the effect of a real surface is ignored. For $D_{(r)}$ the following relation is applied[1]:

$$D_{(r)}(x,E,\cos\phi) = \eta_{(r)}(E) A(x,\cos\phi) \ , \tag{5}$$

where $\eta_{(r)}(E)$ is the total amount of energy deposited in electronic excitation by recoiling target atoms and $A$ some function to be constructed from the moments over $D_{(r)}$. $\eta_{(r)}(E)$ is found using a method proposed in a previous paper.[1] For the higher-order moments over $D_{(r)}$ necessary for the construction of $A$, the damage moments tabulated by Winterbon[7] are used. This seems to be justified since the low-order damage distribution moments show only a small deviation from the corresponding properties of $D_{(r)}$.[3,8]

Since energy transport by excited target electrons is ignored, $D_{(p)}$ has a discontinuity at the target surface. If scattering of the ions is neglected $D_{(p)}$ has the form

$$D_{(p)}(x,E,\cos\phi) = \theta(x)\frac{NS_e(E)}{\cos\phi} \text{ at } x \sim 0 \ , \tag{6}$$

where

$$\theta(x) = \begin{cases} 0, & x < 0 \\ 1, & x \geq 0 \end{cases}$$

and $NS_e(E)$ is the electronic stopping power of the bombarding ions. Using Eqs. (5) and (6) and inserting (4) into (3) one obtains

$$\frac{\gamma(\phi)}{\gamma(0)} = (\cos\phi)^{-1}\left[\frac{D_{(p)}(0,E,1)}{D_{(p)}(0,E,1)+D_{(r)}(0,E,1)}\right] + \frac{A(0,\cos\phi)}{A(0,1)}\left[\frac{D_{(r)}(0,E,1)}{D_{(p)}(0,E,1)+D_{(r)}(0,E,1)}\right] \ . \tag{7}$$

The contribution from the first term in (7) increases as the ratio $D_{(p)}/D_{(r)}$ increases. Thus, in the case of dominating electronic stopping, $D_{(p)} >> D_{(r)}$, an inverse cosine dependence is obtained. For comparable nuclear and electronic stopping and, even more important, for dominating nuclear stopping also the contribution from the second term has to be taken into account. Then, there is no explicit angular dependence as in the case of dominating electronic stopping. It varies with ion energy and depends on (1) the actual ratio of $D_{(p)}/D_{(r)}$, and (2) the actual dependence of $A(0,\cos\phi)$ on $\phi$. In the calculations a Gaussian approximation is made for $A(\cos\phi)/A(0,1)$, i.e., moments up to the second or-

der are taken into account. This gives

$$\frac{A(0,\cos\phi)}{A(0,1)} = \left[\cos^2\phi + (1-\cos^2\phi)\frac{\langle y^2\rangle}{\langle \Delta x^2\rangle}\right]^{-1/2} \exp\left[\frac{\langle x\rangle^2}{2\langle \Delta x^2\rangle}\left[1+\frac{\cos^2\phi\langle \Delta x^2\rangle}{(1-\cos^2\phi)\langle y^2\rangle}\right]^{-1}\right], \tag{8}$$

where $\langle x\rangle$ is the average depth, $\langle \Delta x^2\rangle^{1/2}$ the width, and $\langle y^2\rangle^{1/2}$ the transverse width of the distribution.

## VI. COMPARISON BETWEEN THEORY AND EXPERIMENT

The slowing-down process for 30–400-keV protons and helium ions in copper is dominated by electronic stopping. Thus, the recoil-induced distribution, $D_{(r)}$, can be neglected compared to the primary distribution, $D_{(p)}$. According to Eq. (7), this gives an inverse cosine dependence of the electron yield, which is in excellent agreement with experimental results (Figs. 1 and 2). For neon, argon, krypton, and xenon ions both terms in Eq. (7) have to be considered. In the calculations the nuclear stopping power according to Lindhard *et al.*[9] is applied. The electronic stopping power used is of the form

$$NS_e(E) = KE^{1/2} \tag{9}$$

with $K$ values determined from Brice's stopping-power formula,[10,11] which in the energy range studied, for the ion-target combinations considered, can be rather well approximated by (9). From Eqs. (6), (7), (8), and (9) the following equation for the angular dependence of $\gamma$ is obtained:

$$\frac{\gamma(\phi)}{\gamma(0)} = \left\{(\cos\phi)^{-1}KE^{1/2} + \frac{\exp((\langle x\rangle/2\langle \Delta x^2\rangle)\{1+[\cos^2\phi/(1-\cos^2\phi)]\langle \Delta x^2\rangle/\langle y^2\rangle\}^{-1})}{[\cos^2\phi+(1-\cos^2\phi)\langle y^2\rangle/\langle \Delta x^2\rangle]^{1/2}} \times \frac{\eta_{(r)}(E)\exp(-\langle x\rangle^2/2\langle \Delta x^2\rangle)}{(2\pi\langle \Delta x^2\rangle)^{1/2}}\left[1-\frac{\Gamma}{6}\left[\frac{\langle x\rangle^3}{\langle \Delta x^2\rangle^{3/2}}-3\frac{\langle x\rangle}{\langle \Delta x^2\rangle^{1/2}}\right]\right]\right\} \times \left\{KE^{1/2}+\frac{\eta_{(r)}(E)\exp(-\langle x\rangle^2/2\langle \Delta x^2\rangle)}{(2\pi\langle \Delta x^2\rangle)^{1/2}}\left[1-\frac{\Gamma}{6}\left[\frac{\langle x\rangle^3}{\langle \Delta x^2\rangle^{3/2}}-3\frac{\langle x\rangle}{\langle \Delta x^2\rangle^{1/2}}\right]\right]\right\}^{-1}, \tag{10}$$

where $A(0,1)$ is approximated by an Edgeworth expansion including moments up to the third order and $\Gamma$ is the skewness of $D_{(r)}$.

In order to facilitate the comparison with experimental data the theoretical curves, calculated form Eq. (10), are fitted by a relation

$$\frac{\gamma(\phi)}{\gamma(0)} = (\cos\phi)^{-z}, \quad \text{for } 0°\leq\phi\leq 60° . \tag{11}$$

The fit is not applied to $\phi > 60°$ as the theory is inapplicable at glancing incidence since the target is treated as an infinite medium.

Figures 8 and 9 show the experimental and theoretical values of $z$ versus ion energy for xenon and krypton ions and argon and neon ions, respectively. The agreement is good, except for 40-keV xenon ions, where the theory gives a somewhat lower value than obtained experimentally. A direct comparison between measurements and theory is given in Fig. 10 for 230-keV krypton ions.

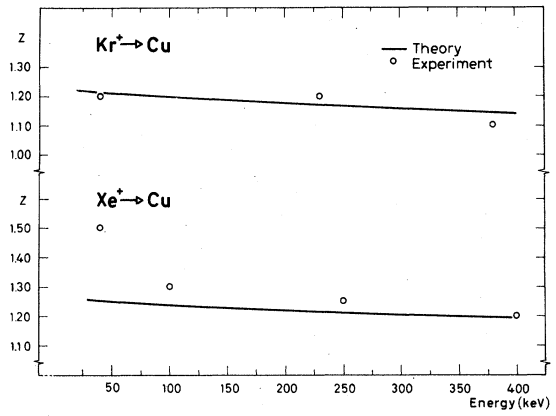


FIG. 8. Extracted fitting parameter, $z$, as a function of ion energy for xenon and krypton ions.

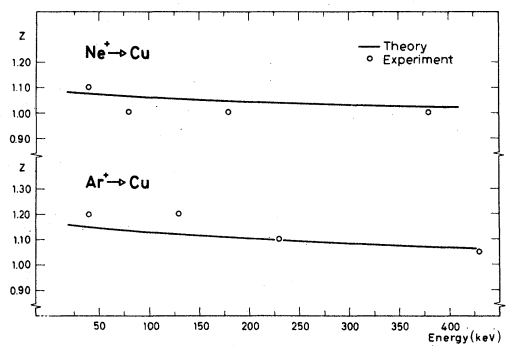


FIG. 9. Extracted fitting parameter, $z$, as a function of ion energy for argon and neon ions.

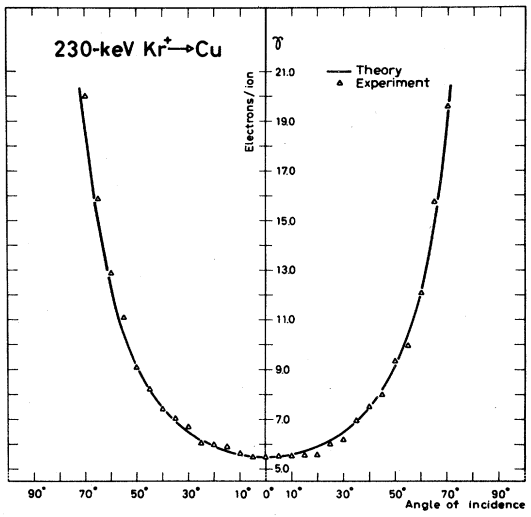


FIG. 10. Secondary-electron yield vs the angle of ion incidence for 230-keV krypton ions.

## VII. DISCUSSION

### A. Light-ion bombardment

The discrepancy between theory and measurements which occurs at $\phi \gtrsim 50°$ for 30-keV protons and 40-keV helium ions is probably due to an increased probability of backscattering at large angles of incidence. The assumption concerning neglecting ion scattering when calculating $D_{(p)}$ breaks down. The effect becomes important mainly at low energies, as the nuclear collision cross section increases with decreasing energy. The backscattered ions may penetrate the surface region important for the secondary electron emission process in both the forward and backward directions. This gives a larger amount of energy deposited at the target surface than estimated by Eq. (6), and thus an enhancement in the yield occurs.

### B. Medium- and heavy-ion bombardment

One possible explanation for the deviation from theory for 40-keV xenon ions may be that the electronic stopping is overestimated, i.e., the $D_{(p)}$ value is too large. This conclusion was also made from measurements of the energy dependence of the electron yield.[1] Furthermore, similar results have been reported by other authors.[12] The present theory cannot explain the maximum in the yield at $80° \lesssim \phi \lesssim 85°$ for 40-keV ions of argon, copper, krypton, and xenon, as the effect of a real target surface is ignored. In the analogous case for the sputtering process two mechanisms have been proposed to explain the maximum. These may also be applied to the electron emission process.

(1) At angles of incidence of close to 90° the ion beam may be deflected from the target surface by a mechanism similar to planar channeling in crystals. This surface effect is due to a potential barrier constituted by a collective action of target atoms at the surface. Since the ions are deflected at the surface, only a small part of their kinetic energy is transferred to target electrons, giving a decrease in the number of emitted electrons. Witcomb[13] has applied Lindhard's analysis of directional effects in the penetration of charged particles through crystal lattices[14] to determine the angle corresponding to the maximum sputtering yield, $\hat{\phi}$. He arrives at the expression

$$\hat{\phi} = 90° - \frac{21.175}{d(Z_1^{2/3} + Z_2^{2/3})^{1/2}} \times \left[ \frac{Z_1 Z_2 (Z_1^{2/3} + Z_2^{2/3})^{3/2}}{N^{2/3} E} \right]^{1/4}, \quad (12)$$

where $N$ is the number of target atoms per unit volume and $d$ the pertinent atom separation in the target lattice, both in units of nm. $E$ is the ion energy in eV and $Z_1$ and $Z_2$ are the atomic numbers of the ions and target atoms, respectively.

In Table I the measured values of $\phi$ corresponding to the maximum electron yield are compared with the calculated values of $\hat{\phi}$. A fair agreement is obtained, but the calculated values are about 3° lower than the measured ones. However, objections can be made to this explanation since it requires an ordered surface structure. This requirement may not be fulfilled, as at glancing incidence a large surface area, consisting of many grains oriented in different directions, is hit by the ion beam. This is emphasized by the difficulty in deciding the appropriate lattice spacing, $d$, to be used in Eq. (12).

TABLE I. The calculated values of $\hat{\phi}$, with $d$ equal to the closest packing target atom spacing, compared with the measured values of $\phi$ corresponding to maximum electron yield for 40-keV ions.

| | Target: Cu | |
|---|---|---|
| Ion | Calculated value of $\hat{\phi}$, with $d = 0.255$ nm (deg) | Measured $\phi$ value at maximum electron yield (deg) |
| Ne | 81.7 | ~85 |
| Ar | 80.6 | 83 |
| Cu | 79.6 | 82 |
| Kr | 79.1 | 82 |
| Xe | 78.1 | 80 |

(2) A second and perhaps more probable explanation may be that at $\phi$ close to 90° the collision cascades are located so close to the target surface that they are not fully developed.[15] Unfortunately, there exist no quantitative theoretical estimates for this effect.

## VIII. CONCLUSIONS

The idea of splitting the kinetic emission of electrons into two contributions, which exhibit different dependences on the angle of ion incidence, is shown to give good agreement between theory and experiments. In particular, for comparable nuclear and electronic stopping and, even more important, for dominating nuclear stopping the recoil-induced excitation of target electrons is found to be of crucial importance for the angular dependence of the electron yield. Further work is required for the explanation of the secondary electron yield maximum at glancing incidence.

## ACKNOWLEDGMENTS

The authors are indebted to Professor O. Almén and Professor G. Andersson for their interest in this work, to J. Jacobsson for assistance with the experimental work, and to M. Soondra for his excellent figures. Special thanks are also due to Professor P. Sigmund, Odense University, Denmark, and to Dr. J. Schou, Risö National Laboratory, Denmark, for many stimulating discussions. Financial support was received from the Swedish Natural Science Research Council, the Swedish Board for Technical Development, Wilhelm och Martina Lundgrens Vetenskapsfond and Fonden för främjande av ograduerade forskares vetenskapliga verksamhet.

[1]G. Holmén, B. Svensson, and A. Burén, Nucl. Instrum. Methods 185, 523 (1981).
[2]G. Holmén, B. Svensson, J. Schou, and P. Sigmund, Phys. Rev. B 20, 2247 (1979).
[3]J. Schou, thesis (University of Copenhagen, 1979) (unpublished); and Phys. Rev. B 22, 2141 (1980).
[4]G. Holmén, E. Kugler, and O. Almén, Nucl. Instrum. Methods 105, 545 (1972).
[5]G. Holmén and P. Högberg, Radiat. Effects 12, 77 (1972).
[6]G. Holmén, B. Svensson, and A. Burén, in *Proceedings of the Seventh International Conference on Atomic Collisions in Solids, Moscow,* edited by A. Tulinov *et al.* (Moscow State University Publishing House, 1980), Vol. 2.
[7]K. B. Winterbon, *Ion Implantation Range and Energy Deposition Distributions* (Plenum, New York, 1975), Vol. 2.
[8]B. Svensson (unpublished).
[9]J. Lindhard, V. Nielsen, and M. Scharff, K. Dan. Vidensk. Selsk. Mat.-Fys. Medd. 36, No. 10 (1968).
[10]D. K. Brice, Phys. Rev. A 6, 1791 (1972).
[11]D. K. Brice, *Ion Implanatation Range and Energy Deposition Distributions* (Plenum, New York, 1975), Vol. 1.
[12]C. D. Moak, B. R. Appleton, J. A. Biggerstaff, S. Datz, and T. S. Noggle, in *Atomic Collisions in Solids,* edited by S. Datz *et al.* (Plenum, New York, 1975), Vol. 1.
[13]M. J. Witcomb, Radiat. Effects 27, 223 (1976).
[14]J. Lindhard, K. Dan. Vidensk. Selsk. Mat.-Fys. Medd. 34, No. 14 (1965).
[15]I. N. Evdokimov and V. A. Molchanov, Can. J. Phys. 46, 779 (1968).